Development of a Molecularly Imprinted Polymer for Use in Biomolecule Detection

Author: Arielle Cimeno

Development of a Molecularly Imprinted Polymer for Use in Biomolecule Detection

Scholar of the College Thesis Submitted by Arielle Cimeno
Advisors:
Prof. Thomas Chiles
Prof. Michael Naughton
Dr. Dong Cai
Arts and Sciences Honors Program
Biology Department
2009

Abstract

Molecular recognition is an important area of research as it has far reaching applications in sensors, molecular separations, and medicine. Molecularly imprinted polymers offer an option for developing high resolution tools of detection that are both selective and sensitive. As a platform, carbon nanotubes offer a highly conductive surface and their growth and unique magnetic properties can be manipulated for our purposes. Such carbon-nanotube based sensors can afford high sensitivity, while molecular imprinting provides the selectivity of detection with the flexibility of fabrication. In order to fabricate a molecular imprint, monomeric compounds are polymerized in the presence of a target molecule of interest, which acts as the template. Once the template molecule has been removed an imprint capable of "recapturing" the target molecule is left behind. In this work we used cyclic voltammetry as a means of depositing polymer coatings doped with a target molecule. We fabricated a molecularly imprinted polymer sensor specific for ferritin using polyphenol as the polymer. The development of our imprint was monitored based on changes in impedance levels calculated by electrochemical impedance spectroscopy. After depositing ferritin-doped polyphenol layers we evaluated the effectiveness of different eluant solutions. Ultimately, deionized water was determined to be the developing solution of choice because it effectively removed the ferritin while not compromising the integrity of the remaining polymer coating. The sensor was capable of detecting ferritin at a concentration of $1x10^{-9}$ g/L (1 pg/mL). In parallel we evaluated the stability of the polyphenol coating.

Acknowledgements

First I would like to thank Prof. Chiles for agreeing to let me work in his lab on this project. I appreciate his ability to find the time despite his many other responsibilities to read and review my thesis as well as to listen to all of my concerns along the way. Without his help and insistence I would not have undertaken an Advanced Independent Research Project, and I certainly would not have produced as well written of a thesis. Finally, I have greatly enjoyed the perpetual comic relief his direct and candid personality constantly provides.

I am also grateful to Dong Cai who cheerfully and carefully taught me about all aspects of the project and the many techniques needed along the way. Additionally, he never got upset at my repeated questions, and was understanding of my busy schedule.

I would like to thank Prof. Naughton for agreeing to be my second reader, and for providing conciseness, clarity, and sanity to all of the group meetings. Also, I greatly respect his extremely clear and logical thinking which I can only hope to imitate someday.

Thanks also goes out to Lucy for guiding me through the EIS system and valuing my input and ideas at each step, and to the other members of the Chiles lab who were considerate of me popping in and out and showed me where the most basic of supplies were.

I would like to most sincerely thank Patrick Behrer, Rob Bell, Kristen Donohue, and Victor Simoes for reading through my thesis. Between the four of them they provided advice on every aspect from organization, to the actual science, to the grammatical composition. I thank them for agreeing to read something they didn't understand and probably didn't want to.

Last, but certainly not least, I would like to thank Tim Kirkpatrick for convincing me to ask Prof. Chiles and Dong to work with them, and for his constant reassurances that I was indeed smart enough to do this work and anything else that I might put my mind to in the future.

Table of Contents

List of Figures

Introduction

The ability to recognize biomolecules is frequently harnessed in nature from enzyme and substrate interactions to antibody and antigen molecules. Traditionally, biosensors have made use of these enzymes, antibodies, and receptor molecules as the primary recognition component. While successful, there are certain limitations when using biomolecules in sensors; mainly that they have limited stability and can be damaged by harsh conditions. Also, new demands and opportunities in the areas of clinical diagnostics, food analysis, and detection of illicit drugs and chemical warfare agents often necessitate detection of species for which there is no naturally occurring recognition molecule[1]. For such purposes there is interest in creating synthetic receptors capable of recognizing unique target molecules.

One method that has received a lot of attention is the development of molecularly imprinted polymers (MIPs), sometimes dubbed "synthetic antibodies"[2]. These are essentially polymer molds that have specificity for a certain target molecule and increased stability over biological agents due to polymer cross-linking[1]. Fabrication of an MIP usually follows either a noncovalent or covalent deposition method, though there have been limited reports of spin coated[2] and spray coated[3] polymers. The noncovalent, or self assembly, method is essentially a two dimensional version of molecular imprinting and involves in situ formation of a self assembled monolayer (SAM) on the sensor surface[4]. Commonly thiol chain molecules are used with a gold surface and the introduction of a foreign molecule will cause a void in the SAM that is specific in size for the molecule that created it[5]. Several researchers have had success with this method and have reported highly sensitive detection of small molecules such as cholesterol[6], phenylalanine[7], and methyl viologen[8]. Detection of small molecules like these is now considered routine, but molecular imprinting can be applied to many targets including larger and more complex ones such as proteins and cells which still present some challenges due to their size[9]. Despite the challenges SAM based sensors that effectively detect streptavidin[10], hemoglobin[11], and E. coli[12] have been reported.

The covalent method involves copolymerization of the polymer monomers and the target molecule which acts as a template for imprint development. The monomers and the imprint molecule form complexes that allow for various functional groups to be held in place by the cross-linked polymer. Once the template molecule is removed, usually by washing with electrolyte[7] or detergent[9] solutions, the voids that remain are binding sites for the target that are

specific in size and shape[1]. The majority of molecularly imprinted polymers that have been synthesized are done so via a radical polymerization mechanism[1, 13]. Sensors using MIPs fabricated via electropolymerization have been made with specificities for cholesterol[14], sorbitol[15], glucose[16], and protease[17] among others.

Both the noncovalent and covalent methods have their advantages. SAMs are generally easier to generate, do not require reagents capable of polymerization, and allow for easier template removal. Meanwhile, it is possible that covalent methods give more uniform binding sites due to the regularity with which the polymer and template molecules will align compared to self assembly which is a more random process.[18] Also the efficiency, how much template molecule needs to be used, should be greater with the polymerized method[19]. In order to get the advantages of both methods it is possible to use both to generate a more complex MIP[7]. Either way, the binding sites generated by imprinting have affinities comparable to those of antibody antigen systems causing MIPs to be nicknamed "antibody mimics"[20]. MIPs have applications outside of sensors and have been used for stationary phases in HPLC[21], thin -layer chromatography[21], capillary electrochromatography[22], and solid phase extraction[23], where they have selectivities capable of distinguishing between enantiomers[24].

The selection of polymer to be used depends on the polymerization conditions, template molecule, and preferred means of detection. Some polymers that have been used include polypyrrole (PPy)[25-27], polyphenol (PPn)[7, 10, 13, 16], poly(*o*-phenylenediamine) (PPD)[15, 28], and poly(2-macaptobenzimidazole) (PMBI)[14]. In order for MIPs to be successfully integrated into sensors some kind of measurable signal must be generated upon binding of the target molecule. Some possibilities include fluorescence[29], amperometry[21], ellipsometry[30], voltammetry[31], and quartz crystal microbalance[28]. The first integrated sensor using an MIP was a capacitance sensor[32]. Electrochemical tests including cyclic voltammetry and electrochemical impedance spectroscopy are very popular, because it has been demonstrated that when charged proteins are trapped by the MIP on top of a metallic conductor there is a change in the surface potential, which can be measured potentiometrically using a reference electrode immersed in the same solution[11]. For use in electrochemical experiments the main decision is whether to use a conducting or non-conducting polymer as there are advantages and disadvantages to each. If the polymer is deposited electrochemically such as through cyclic voltammetry, a nonconductive polymer will initiate a self limiting reaction since the deposition will stop once a thickness has

been reached that insulates the underlying conductive electrode surface[7]. In such cases the thickness of the polymer coating has a defined limit. With a conductive polymer deposition will occur in theory infinitely and the thickness of the polymer coating can be manipulated based on the time and conditions of the deposition reaction. The conductivity of the polymer also influences the detection methods available, as changes in impedance can more easily be detected with a non-conductive polymer. When both the polymer and target molecule are electrically inactive ferrocene carboxylic acid (FCA) is used to generate a signal[14].

Currently there is movement to fabricate miniaturized MIP biosensors that would afford greater sensitivity and could be incorporated into arrays that would simultaneously detect multiple targets[33]. To this end carbon nanotubes (CNTs) have been identified as a superior sensor scaffold due to their unique geometry, electrical, mechanical and structural properties as well as their growth manipulability[26]. CNTs can also display metallic, semiconducting, and superconducting properties, and have the largest elastic modulus of any known material[34]. One characteristic that makes CNTs particularly useful in nanoscale sensors is their high sensitivity to surface adsorbates[35]. Two types of carbon nanotubes, single walled carbon nanotubes (SWCNTs) and multi walled carbon nanotubes (MWCNTs), exist. SWCNTs have a cyclindrical structure similar to a single sheet of graphite rolled into a tube. MWCNTs contain several layers of grapheme cylinders assembled like nested coffee cups with an interlayer spacing of about 3.4 Å[36]. MWCNTs are highly conductive and the incorporation of a nickel particle to their tips along with their curved outer wall structure make them magnetic and increase the magnetic field and therefore faradic current generated around the CNT. When grown via plasma enhanced chemical vapor deposition (PECVD) CNT arrays with lower site density are obtained creating enough spacing between CNTs to avoid physical contact between each other[37].

A potential limitation of vertically grown aligned MWCNTs is that while they have been shown useful for amperometric sensors[38] they have also been shown to bend and stick together in liquid environments due to surface tension[25]. Two methods to circumvent this problem have been developed. First, coating of CNTs electrochemically with PPy and other polymers stabilizes them. Also the relatively large surface area of CNTs allows lots of PPy deposition at low thickness[25]. Second, CNT arrays can be embedded into photoresists or spin on glass[39]. Once embedded the arrays can be polished leaving only the tips exposed[40]. While this stabilizes

the CNTs it greatly reduces the available sensor surface area. However, successful sensors have been fabricated using this design[41].

In this work we design and fabricate a molecularly imprinted nanoscale sensor on top of aligned CNTs. For this, polyphenol is used as the polymer and ferritin as the target molecule. We discuss the considerations and effectiveness of our chosen design and attempt to evaluate the efficiency of different developing solutions to generate an MIP. Finally, we test the quality of the imprint's sensitivity. We also investigate the stability of the polyphenol coating under various conditions.

Materials and Methods

CNT Array Production

CNTs were grown in patterned arrays on silicon substrates coated with metal, typically titanium. Using a sphere monolayer masking technique nickel dots were deposited in arrayed hexagonal patterns on the substrate. These dots acted as the catalyst for CNT growth via PECVD[43]. Arrayed CNT samples were obtained from Dr. Huaizhou Zhao and Trilochan Paudel in the BC Physics department. The CNTs were typically 2 μm in length and 200 nm in diameter.

Fabrication of Sample Structure

Arrayed CNT samples were spin coated with SU8, a negative photoresist. Spin coating was carried out under the following conditions: 9 sec. at 700 rpm followed immediately by 30 sec. at 3000 rpm which completely submerged the CNTs. After spinning the sample was soft baked at 100°C for 5 min. The sample was then placed under UV light for 3 minutes. Following UV light exposure the sample was hard baked for 2 min. at 150°C then overnight at 200°C.

Vibrational polishing was used to polish away some of the SU8 in order to expose the tips of the CNTs using a VibroMet 2 Vibratory Polisher (Buehler). Polishing was conducted at 70% amplitude (max horizontal motion is 7200 cycles per second). Length of time for polishing was determined based on Scanning Electron Microscopy (SEM) images of exposed CNT tips. On average, polishing was carried out for between four and nine hours.

Additional verification of exposed CNT tips as well as cleanliness of the sample surface was conducted via cyclic voltammetry with FCA to produce a characteristic "duck" under the following conditions: scan range 0.6 to -0.6 V, scan rate 100 mV/sec, step size 5 mV, cycles 3. All electrochemical tests were conducted with a Gamry PC4/750 that was linked to a Pentium III computer system. Gamry Instruments Framework and Gamry Echem Analyst software were used for recording and analyzing data. An Ag/AgCl electrode was used as the reference electrode and a platinum wire as the counter electrode.

Polymer Deposition

The CNT sample was connected electrically to the working electrode via copper wire attached with silver paint. Initially PPn deposition was carried out via cyclic voltammetry under

the following conditions; scan range 0 to 0.9 V, scan rate 50 mV/sec, step size 2 mV, 5 cycles, and occurred only on the exposed CNT tips. The concentration of phenol was 5 mM in PBS. For imprinted samples the phenol solution was doped with ferritin at a concentration of 10 μg/μL.

Later Electrochemical Impedance Spectroscopy (EIS) was employed in a multi-step approach to deposit PPn. First cyclic voltammetry under the above conditions was conducted to verify the cleanliness of the sample surface. Then Potentiostatic EIS under the following conditions; initial frequency 1x 10^6 Hz, final frequency 0.1 Hz, AC voltage 10 V, and DC voltage 0.3 V, established a baseline level of impedance for the bare CNT sample. Deposition occurred via single frequency EIS with AC voltage of 10 V, DC voltage 0.5 V, repetition time of 0.04 minutes, and total time of 0.2 hours with a solution of ferritin in PBS. This was followed by cyclic voltammetry under the following conditions: scan range 0 to 0.9 V, scan rate 50 mV/sec, step size 2 mV, 5 cycles.

Deposition was confirmed by the decreasing signal strength of the cyclic voltammetry plot as well as by cyclic voltammetry with FCA under the following conditions: scan range 0.6 to -0.6 V, scan rate 100 mV/sec, step size 5 mV, cycles 3. Potentiostatic EIS was also conducted under the above conditions. Further verification of PPn deposition was obtained through SEM and Transmission Electron Microscopy (TEM) images.

Ferritin Removal

Several solutions were tested to remove bound ferritin from PPn. These included 50 mM NaH_2PO_4, ethanol, 1% SDS, 1% Trition x-100, 0.1% Tween-20, 1% NP-40, 3% SDS / 1% Triton x-100, 10% SDS, 10% SDS / 0.5% acetic acid, 10% SDS / 1% acetic acid, 10% SDS / 2% acetic acid, 10% SDS / 5% acetic acid, 10% SDS / 10% acetic acid, and deionized water. Solutions were stirred and/or heated for various times and at different temperatures, respectively.

Imprint Verification

The presence of an imprint was verified in three ways. First, cyclic voltammetry measurements were carried out under the following conditions: scan range 0.6 to -0.6 V, scan rate 100 mV/sec, step size 5 mV, cycles 3. Second, the presence of the imprint was verified by changes in impedance as measured by Potentiostatic EIS under the following conditions: initial

frequency 1x 10^6 Hz, final frequency 0.1 Hz, AC voltage 10 V, and DC voltage 0.3 V. Third, the imprint was visualized under TEM.

Evaluation of PPn Stability

Non-imprinted, non-ferritin doped PPn was tested to evaluate its stability under varying pH, solvents (methanol, ethanol, acetone), temperatures (up to 100°C), and surfactants (1% SDS, 1% Trition x-100, 0.1% Tween-20, 1% NP-40). Multiple combinations of SDS / acetic were tested as well. These controls were carried out using the same or similar samples to the ones used for experimental tests and were prepared in the same way. The single frequency EIS step used PBS without ferritin. All other concentrations and conditions were the same.

Evaluation of Imprint Quality

The quality of the imprint was evaluated based on its ability to recognize ferritin. Ferritin solutions with concentrations ranging from $1x10^{-4}$ g/L to $1x10^{-9}$ g/L were reintroduced to the sensor after imprint development. Measurements of the impedance were conducted using Potentiostatic EIS under the above conditions.

Results

Design

Figure 1 represents a schematic of the proposed sensor. Vertically grown arrayed CNTs (brown) would be embedded in SU8 (orange) and vibrationally polished to expose the tips. Phenol doped with ferritin (gray) would be electrochemically polymerized and deposited onto the exposed CNT tips. The ferritin would then be washed away from the polymer leaving an imprint (black). Electrochemical measurements would be used to evaluate the sample before and after each step.

Component Selection

The overall idea was to use vertical arrays of CNTs as the working electrode in a standard two electrode system and coat them with a polymer as previously described[25]. As it would be necessary to have the surface of the CNTs available for deposition it seemed reasonable to use the entire CNT, tip and sides, in order to maximize the available surface area. However, in other reports[39, 40] it was shown that CNTs are likely to clump together once placed in an aqueous environment like the situation envisioned for our electrochemical measurements. Another concern was handling of the samples, as CNT arrays are easily damaged, i.e. the CNTs break off from the underlying substrate if they are touched or dropped. Thus, to ensure easier handling and minimize potential damage to the samples it was decided to embed and polish the CNT arrays as already discussed. An added benefit of this design is that embedding would insulate the underlying substrate and guarantee that the only signal generated originated from the CNTs. Additionally, it is difficult to visualize the polymer coating near the base of the CNTs, and voids or discontinuities in the coating would lead to current leaks that could generate false results. By embedding the CNTs these problems are eliminated. Moreover, the flat surface can be easily cleaned before the polymer is deposited. Then after the sample has been used once, additional polishing can remove whatever was deposited (polymer and proteins) as well as a slight additional amount of the CNT and matrix, therefore making the sample multiuse.

Several considerations went into choosing SU8 as the resist for embedding. First, it is a negative photoresist meaning that exposure to UV light causes cross-linking and it assumes a very hard, glass-like consistency. After UV exposure the process is irreversible guaranteeing

that nothing will damage the resin and consequently the CNT array within it. This is the opposite of positive photoresists which break down under light exposure. By choosing a negative photoresist we had a relatively easy way to ensure a sturdy coating that would not break down under normal conditions and exposure to light. SU8 also dries quickly, so once the spin coating of the sample was completed there was little chance of damaging the coating or making it uneven by handling. Like most negative photoresists, SU8 is non-conductive providing an inert surface that would not interfere with measurements. While SU8 is resistant to most chemical means, including acids, bases, and common solvents, it is not completely resistant to mechanical means so it can be polished away. This is necessary to expose the tips as our current procedure would not allow us to spin on a layer of SU8 that is thinner than the length of the CNTs. It also means that if the sample became dusty or dirty, or if it was suspected from cyclic voltammetry measurements with FCA that some organic substance had adsorbed onto the surface, it would be possible to clean the sample with acetone and polish remover without damaging the SU8. SU8 is also transparent. The CNT samples diffract light producing an "oil on water" like pattern which could still be seen through the photoresist as a quick way of checking that the sample had not undergone any obvious physical damage and that there were no areas devoid of nanotubes. Finally SU8 is easy to work with and apply via spin coating as it starts as a low viscosity liquid that can be easily spun down to a thin layer.

The Chiles lab had previously worked with PPy deposited on CNT tips. PPy is a conductive polymer and when it was deposited via cyclic voltammetry a ball shape was obtained because continued deposition could take place on top of the already deposited PPy. For development of an MIP a non-conductive polymer was desired so that only a thin film rather than a ball would be deposited on the CNT tips. Phenol (and subsequently polyphenol after polymerization) was chosen as the polymer for the imprint primarily because it was such a non-conductive polymer. A non-conductive polymer would also insulate the below CNTs, signaling when a continuous coating had been deposited. The reaction is self limiting as the PPn will only deposit onto a conductive surface. Once the PPn polymer layer reaches a certain thickness, found experimentally to be approximately 15 nm, the carbon nanotube no longer attracts additional PPn to deposit onto it. This allows for a relatively easy method of evaluation of the polymer coating. A uniform continuous coating will produce a completely insulating layer which can be measured electrochemically. If the PPn layer is undisrupted and thick enough

cyclic voltammetry sweeps will reveal a very low and essentially negligible signal for the recorded current. This presented an advantage because when the polymer and template molecule were co-deposited removal of the template would leave voids on the surface of the polymer film. It was anticipated that the presence of these voids could be detected by an increase in current signal generated, essentially by detecting current leakage through the very thin polymer layer under the imprinted cavity.

Experimental Results

Figure 2 shows the CNT array from directly above (a) and at a 45 degree tilt (b) before and after (c) it was polished. In the polished sample the dark circular areas are the CNTs and the light dots in the center of each one are the nickel particles at the tip of each CNT. The white area between the CNTs is the SU8. As seen, the CNTs are arranged in a hexagonal pattern. This had several advantages, the most practical of which being that the hexagonal pattern served as a marker for judging when the CNTs had been sufficiently polished. If the hexagonal pattern could be seen then all the CNTs were exposed, otherwise insufficient polish yielded only some of the CNTs exposed in an irregular pattern. It was found that samples varied in the amount of time needed for polishing. Most samples needed approximately four hours of polishing, while some required up to nine hours. This is not a large discrepancy due to differing experimental conditions. Continuous polishing was more effective than discontinuous, i.e. one four hour period of polishing accomplished more than four one hour sessions. The samples that required longer polishing times were frequently stopped and checked under SEM. A main concern was not to over polish the samples for two reasons. First if the samples were over polished the CNTs became very short and were coated by only a thin film of SU8. Thus it was possible that there would be current leakages from the substrate through the SU8, and the SU8 was more likely to crack, both of which would lead to inaccurately high current readings and false results. It was also possible in this case that the polymer would deposit on surfaces other than the CNT tips introducing great variety into the samples and making it impossible to compare results between samples and giving inaccurate readings. A second consideration was that after a sample was utilized (an imprint developed on the surface) it could be reused after additional polishing to remove the MIP. Each polishing would wear down the sample so we could only use each sample

a finite number of times, though not over polishing would increase this number. Another contributing factor to the discrepancies in polishing times is that while the same procedure was used for spin coating every sample slight differences in the amount of SU8 applied, the length of time at each temperature, and the amount of time elapsed between steps could contribute to thicker SU8 or a sturdier coating which would necessitate more polish time.

As already mentioned, for the electrochemical deposition and evaluation the polished CNT sample served as the working electrode and the reference electrode was a standard Ag/AgCl electrode. Before depositing any polymer we wanted to make sure that the surface of the sample was clean. This was accomplished through cyclic voltammetry with FCA to observe the plot generated by the bare CNT tips. Figure 3 shows a plot of current versus voltage, the inset is voltage versus time. A clean sample would produce a characteristic "duck" shape as shown. In this plot which progresses from left to right and top to bottom the upward wave is the anodic wave (note the negative I values) which represents the oxidation reaction and the downward wave is the cathodic wave (note the positive I values) which represents the reduction reaction. For a conductive surface (such as the polished CNT tips) this is the expected plot. A reversible reaction will have a "duck" with cathodic and anodic waves of the same magnitude as measured from the initial point on the upward or downward sweep. As expected this plot shows an almost perfectly symmetrical shape indicating that the FCA test is completely reversible, or in other words, has no overall effect on the sample. In the course of experiments all samples were tested in this way before PPn deposition. If the plot revealed a diminished current or unusually shaped graph this indicated the sample was not clean. To clean, the sample was rinsed with acetone and polish remover. FCA testing and cleaning were repeated until an acceptable duck shape was obtained. It was also found that storage of the sample usually necessitated cleaning before use which was always easily accomplished by the above polish remover and acetone treatment. This test also established a baseline current level for the sample.

Cyclic voltammetry was also used to deposit the PPn onto the CNT tips. Figure 4 shows a representative plot obtained for this step. As seen in the plot, there is a large anodic peak on the first cycle but no corresponding cathodic peak. For a standard cyclic voltammetry plot a lack of symmetry indicates an irreversible reaction. The lack of a symmetrical cathodic peak for this reaction indicates that the oxidation of the polymer is irreversible – it has been oxidized and deposited onto the surface of the CNTs. Also of note is the lack of any peaks in the subsequent

cycles. This indicates that no reactions are taking place due to the fact that the CNT tips have been completely covered with PPn during the first cycle. Because the only conductive surface has now been covered by PPn and insulated, the circuit has been disrupted as there is no working electrode visible to the polymer. While it appears that one cycle is enough to coat the CNTs, polymerization reactions are set up to run for five cycles to guarantee that any small areas not covered with PPn during the first cycle were covered on later cycles. To verify that the PPn film was indeed completely insulating, cyclic voltammetry with FCA was conducted as it had been originally to test the cleanliness of the sample. As shown in Figure 5, the current level is very close to zero and there are no visible peaks as would be expected for a non-conductive surface and essentially an incomplete set up (absence of working electrode to the FCA). At first, PPn only films were deposited on several samples to verify the outcome of the deposition as well as to test the polymer stability (described later). For fabrication of an imprinted sample the same deposition procedure was followed, this time introducing ferritin into the PPn solution. Similar plots to the above figures were observed.

In order to verify the deposition, as well as to monitor for the incorporation of the ferritin into the PPn layer, CNTs not embedded into SU8 had PPn deposited onto them under the same conditions. Figure 6 shows the PPn coated CNTs under SEM. As visible from the SEM image the nanotubes are covered in PPn. Unfortunately, for the ferritin doped samples no ferritin molecules were observed incorporated into the PPn coating. To rectify this, the deposition was separated into two steps. First a ferritin only buffered solution was placed on the sample and a voltage was then applied for a brief period of time to oxidize the ferritin. After this, the PPn solution was added into the sample for cyclic voltammetry and the oxidized ferritin was more easily entrapped by the forming PPn layer. Figure 7 shows a TEM image of the PPn coated CNTs obtained after this process. The visible dark spots in the PPn coating correspond to ferritin molecules. Each protein molecule appears to have its own area of space. This is important because should the ferritin all clump together there will not be an imprint of the molecule upon removal but rather large voids that would not be specific to ferritin and thus not valuable for ferritin recognition. From this image it can also be seen that there are ferritin molecules both on the surface of the PPn coating as well as completely trapped within the PPn coating. For MIP development only ferritin molecules that are at least slightly exposed on the surface are likely to be removed from the PPn and will leave behind imprints. It is assumed that molecules

embedded deeper in the coating are unlikely to move around within the polymer. Because ferritin is also non-conductive, it should behave similarly to the PPn insomuch as acting like an insulator. Therefore the presence of additional molecules inside the PPn layer is not a large concern.

A major concern with removing the ferritin from the polymer was the ability to leave the imprint intact and not disrupt the morphology of the polymer. For this reason several types of solutions were tested to determine their compatibility with PPn. The affect of pH, surfactants, organic solvents, and temperature were evaluated. It was determined that methanol and acetone were incompatible solvents with PPn while ethanol was compatible. A solution with a low pH of around 1 was also incompatible with the PPn coating. All of the surfactants tested, Triton x-100, Tween-20, NP-40, and SDS were found to be compatible. Additionally the PPn layer was found to be stable at temperatures up to 100°C. (See Figure 8)

For the first several attempts at removing the ferritin from the PPn, samples not embedded in SU8 were again used so that the results could be visualized under TEM. Three conditions were tested: 50 mM NaH_2PO_4, ethanol, and 3% SDS/1% Trition x-100 solution. TEM images of these three samples were inconclusive, although the 50 mM NaH_2PO_4 and 3% SDS/1% Trition x-100 conditions appeared promising (data not shown).

New polished samples were prepared as discussed above and PPn doped with ferritin was deposited. The following solutions were used in an attempt to generate an imprint in the polymer by removing the ferritin: 50 mM NaH_2PO_4, ethanol, 1% SDS, 1%Trition x-100, 0.1% Tween-20, 1% NP-40, 3% SDS / 1% Triton x-100. In addition, the above solutions were tested with heating and stirring for extended periods of time. If the ferritin was removed it was anticipated that cyclic voltammetry measurements with FCA would show a current intermediate between the level established for a polished polymer free sample and a polymer coated sample. This is shown by a series of blue dots in Figure 9 that are overlaid on the cyclic voltammetry plot of a polymer coated sample before the ferritin has been removed. Unfortunately, an increase in current was not observed after any of the removal procedures. This may be due to the fact that the ferritin was either too tightly bound to the PPn or that there were too few ferritin molecules exposed enough on the surface to come free and the majority of the ferritin was trapped within the PPn.

Alternatively, the level of detection was not sensitive enough to detect and distinguish between the signal generated by the intact ferritin doped PPn layer and the ferritin removed PPn. A new electrochemical system capable of EIS measurements was purchased and used for subsequent experiments.

Samples were spin coated with SU8, polished, cleaned, and coated with ferritin doped PPn in the same way as previously described. However, instead of using cyclic voltammetry with FCA to compare changes in current levels before deposition, after deposition, and after attempted ferritin removal, potentiostatic EIS was used to compare the impedance after each step. Also, a new developing solution of 10% SDS/10% acetic acid was used to remove the ferritin[42]. As seen in Figure 10 there was a noticeable difference after each step. The polished CNT sample (black) showed a low level of impedance as would be expected since the sample was uncoated and the exposed CNT tips are highly conductive. After PPn + ferritin deposition (red) the impedance greatly increased; indicative of a uniform and complete polymer coating. After development with SDS/ acetic acid solution the impedance dropped to a level lower than that of the coated sample but higher than that of the uncoated sample (purple). This intermediate level of impedance is considered the result of small cavities and voids on the surface of the polymer layer resulting from the successful removal of the ferritin. When ferritin was reintroduced to the sample the impedance increased, but did not equal the level observed before the SDS/ acetic acid treatment (green). Two main possibilities exist to explain this result. First some but not all of the imprint sites rebound ferritin molecules. It is highly likely that not every imprint site had a ferritin molecule come into contact with it and/or that when contact was made between a ferritin molecule and an imprint site it was not in the correct orientation. Also given more time it is possible that more sites would become filled and the impedance would increase further. Second it is possible that the acid in the developing solution caused partial deterioration of the polymer. To investigate this possibility additional samples were tested with decreased levels of acetic acid. Also, control samples were tested in solutions of different concentrations following the same procedure but without doping the PPn with ferritin.

Solutions containing 10% SDS and acetic acid concentrations varying from 0.5% to 5% were tested as developing solutions for ferritin doped PPn samples. It was found that for all the samples there was a decrease in impedance after the development process. However, as seen in Figure 11 it was not easy to identify a trend between concentration of acetic acid and change in

impedance. One notable observation was a trend in time used for development. The samples were all tested once after 15 min. and again after an additional 15 min. (30 min. total). It was consistently found that the impedance decreased as the developing time increased leading us to conclude that a longer developing time corresponded to the removal of more ferritin. Also visible in Figure 12 are the traces where no acetic acid and just SDS was used. These traces also show a decrease in impedance from the sample before development, and a further decrease with an extended amount of time for development. This was unexpected as previous cyclic voltammetry measurements with SDS did not show a change in current level after development. However these prior conclusions were not based on EIS measurements but rather on less sensitive cyclic voltammetry tests, so it was possible that SDS alone was an adequate eluant. Second, the concentration of SDS tested before was only as high as 3% compared to 10% SDS employed in this experiment. Therefore the higher concentration may have been more effective at removing the bound ferritin.

The next series of experiments were a set of controls where PPn was deposited without ferritin. These samples underwent the same preparation and deposition procedure and PBS was substituted for ferritin in the single frequency EIS step. It was anticipated that after the samples were developed there would not be a decrease in the impedance because the polymer coating should remain unchanged as there is no ferritin to remove. An experiment using 10% SDS / 5% acetic acid did show a decrease in impedance (data not shown). This verified our hypothesis that the acid in the developing solution was degrading the polymer. Tests with lower acetic concentrations also showed similar decreases in impedance. A final test with 10% SDS and no acetic again showed a decrease in the impedance (data not shown). At this point it was concluded that either the concentration of the SDS solution was too high and it was degrading the polymer coating, or our testing and storage conditions were causing the polymer to deteriorate.

Ultimately it was decided to test deionized water as a developing solution. We observed a decrease in the impedance level for the ferritin doped sample, but no change in the impedance level for the undoped sample as seen in Figure 12. From this we can conclude that deionized water by itself is the best developing solution since it removed the ferritin but did not affect the integrity of the PPn coating. When we tested to see if the sample would detect ferritin we were able to observe a significant increase in the level of impedance when ferritin solutions with a

concentration as low as $1x10^{-9}$ g/L (1 pg/mL) was introduced. From this it was decided that deionized water was successful in removing the ferritin and that it would be the developing solution for any future experiments.

Discussion

In this work we sought to design and fabricate a biosensor, the main component of which was a molecularly imprinted polymer deposited onto a carbon nanotube array. We found that cyclic voltammetry was a successful method for the deposition of PPn and ferritin doped PPn onto CNTs, and that we were able to generate an insulating polymer layer. This polymer layer was found to be stable in a range of temperatures up to 100°C as well as solutions of ethanol and common surfactants including, SDS, Tween-20, Triton x-100, and NP-40. The polymer layer was not stable in solutions of methanol, acetone, or at a low pH (~1). These results led us to use a combination of SDS and acetic acid as the developing solution to remove the ferritin from our polymer. EIS measurements distinguished a significant difference between the impedance of an uncoated CNT sample, a ferritin doped PPn coated sample, and a developed sample. However, further tests indicated damage to the polymer coating during development. Additional experiments allowed us to conclude that the best developing solution would be one of deionized water which would allow for removal of the ferritin while maintaining the integrity of the imprinted polymer. Under these conditions our sensor was able to detect ferritin at a concentration of $1x10^{-9}$ g/L (pg/mL).

The above results demonstrate the successful fabrication of our sensor. While previously discussed works have made use of molecularly imprinted polymers, CNT arrays, photoresist embedding, and electrochemical detection separately, we were able to combine these components into a novel design for a biosensor. We also demonstrated the ability to detect target proteins, in this case ferritin, based on changes in the electrochemical impedance of an imprinted polymer at an extremely low concentration. Previously reported sensors using MIPs have demonstrated sensitivities on the level of μg/mL for small molecules[1, 6, 15] and mg/mL[9] for proteins. Thus the level of sensitivity demonstrated by our sensor is better than these previously reported results by several orders of magnitude. An important next step we are pursuing is evaluating the selectivity of our sensor based on its ability to distinguish between ferritin and other proteins. We expect our sensor to exhibit a high level of selectivity meaning that there will not be unspecific binding of other proteins to the ferritin imprints.

We chose to make a sensor specific to ferritin, a ubiquitous protein in humans and a major site of intracellular iron storage. An iron deficiency can lead to anemia while increased iron levels indicate iron overload disorders. The presence or absence of iron affects the

conformation of the ferritin protein. Having a sensor that will detect the amount of ferritin in a certain conformation (with or without iron) can be used to diagnose iron related illnesses.

Our current design can also be adapted for the creation of MIPs with specificities for other proteins or biological components that currently do not have a naturally occurring recognition molecule. The applications would be far reaching and could include medical diagnostics, detection of biological toxins, and illegal drug screenings.

Figures

Figure 1. Schematic of Proposed Sensor Structure

a)

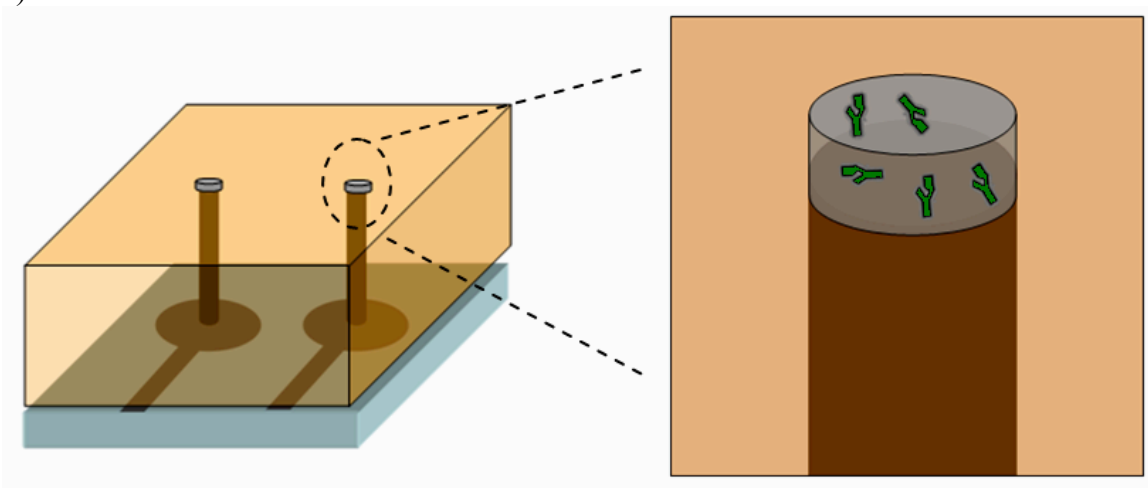

b)

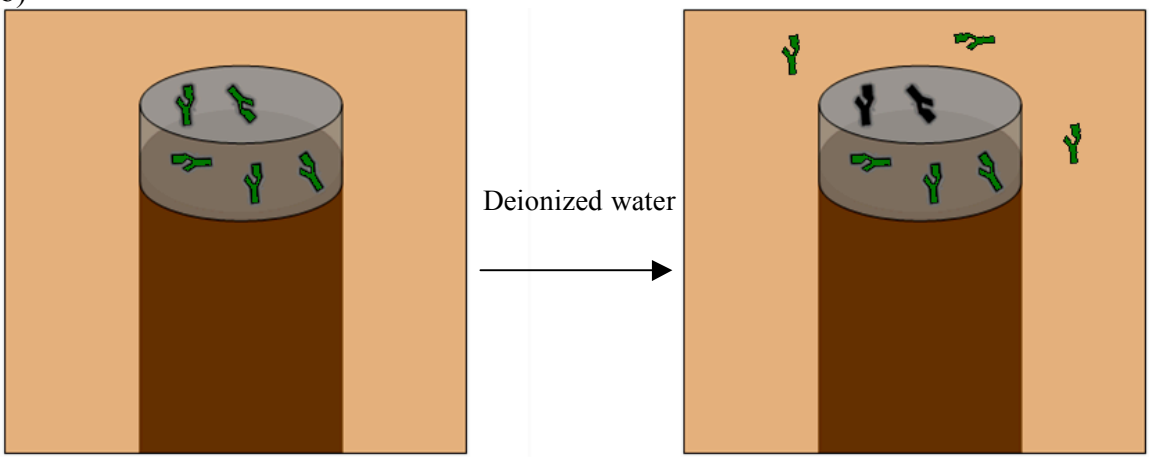

Figure 1. a) The brown represents the carbon nanotubes which are embedded in SU8 (orange) and polished to expose the tips. Ferritin (green) doped polyphenol (gray) is deposited on the tips. b) After ferritin removal via washing with deionized water an imprint (black) is left.

Figure 2. SEM Images of Carbon Nanotube Arrays

a)

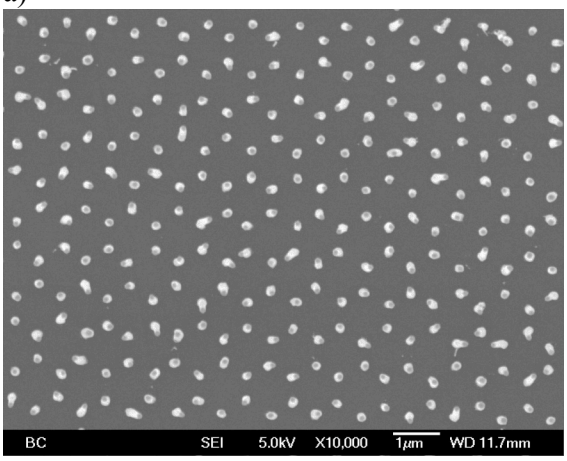

b)

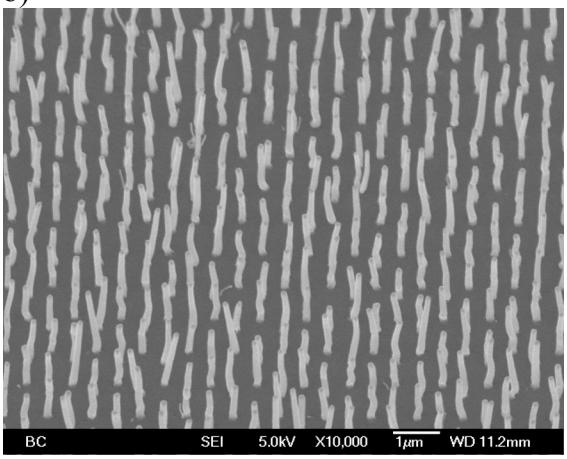

c)

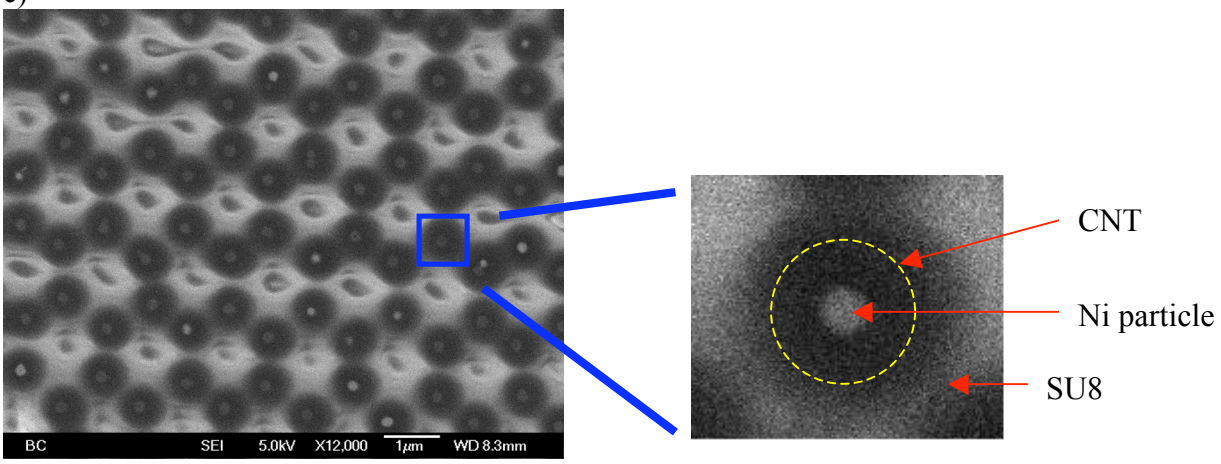

Figure 2. a) The CNT array from above before embedding in SU8. b) The same array at a 45 degree tilt. The CNTs were typically 2 μm in length and 200 nm in diameter.
c) The array after it has been embedded in SU8 and polished completely revealing the hexagonal arrangement of the carbon nanotubes. Note the 1 μm scale bars.

Figure 3. Cyclic Voltammetry Plot of Polished Carbon Nanotube Array

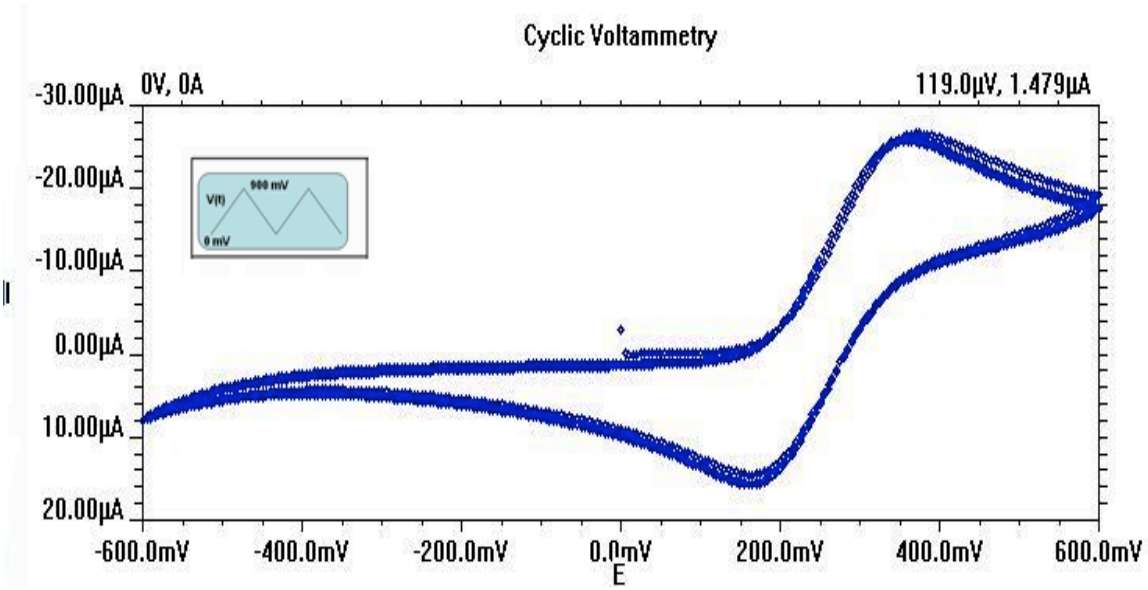

Figure 3. A standard "duck" shaped plot where the upward peak is the anodic peak (oxidation reaction) and the downward peak is the cathodic peak (reduction reaction). The symmetry of the peaks indicates that the reaction with FCA is reversible and has no net effect on the sample. The inset displays the voltage applied as a function of time.

Figure 4. Cyclic Voltammetry Plot of Polyphenol Deposition

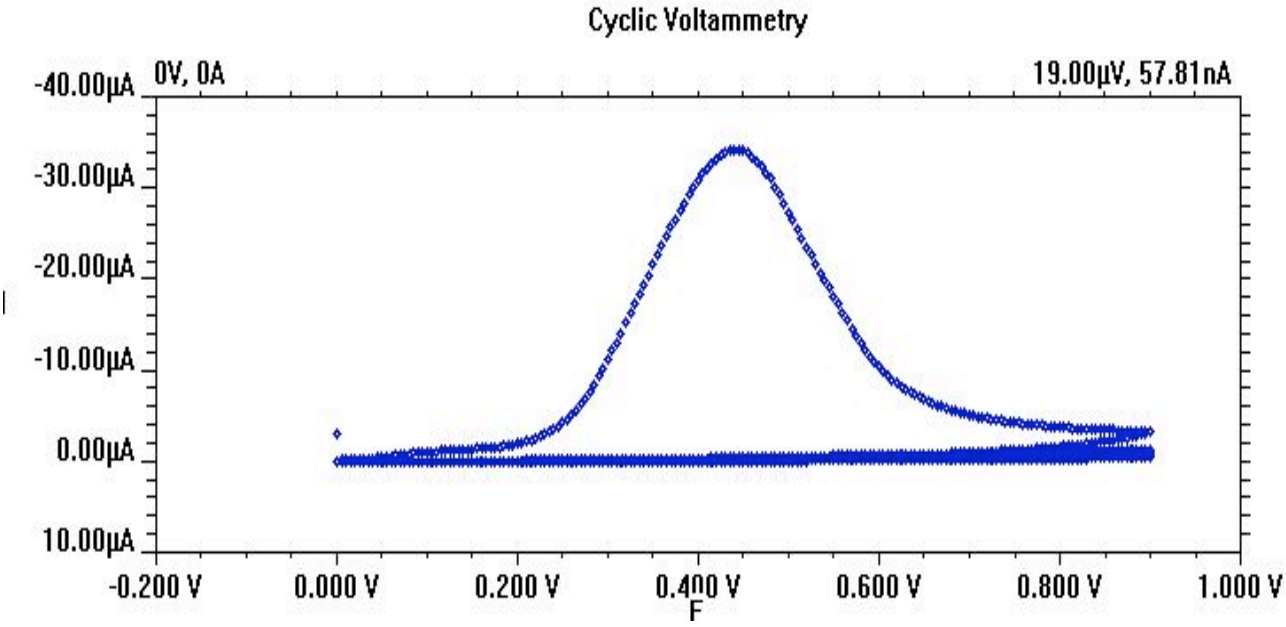

Figure 4. A single large anodic peak is visible. The lack of a symmetrical cathodic peak signals that the reaction is irreversible. The lack of any peaks after the first cycle indicates that the deposition has gone to completion.

Figure 5. Cyclic Voltammetry Plot after Polyphenol Deposition

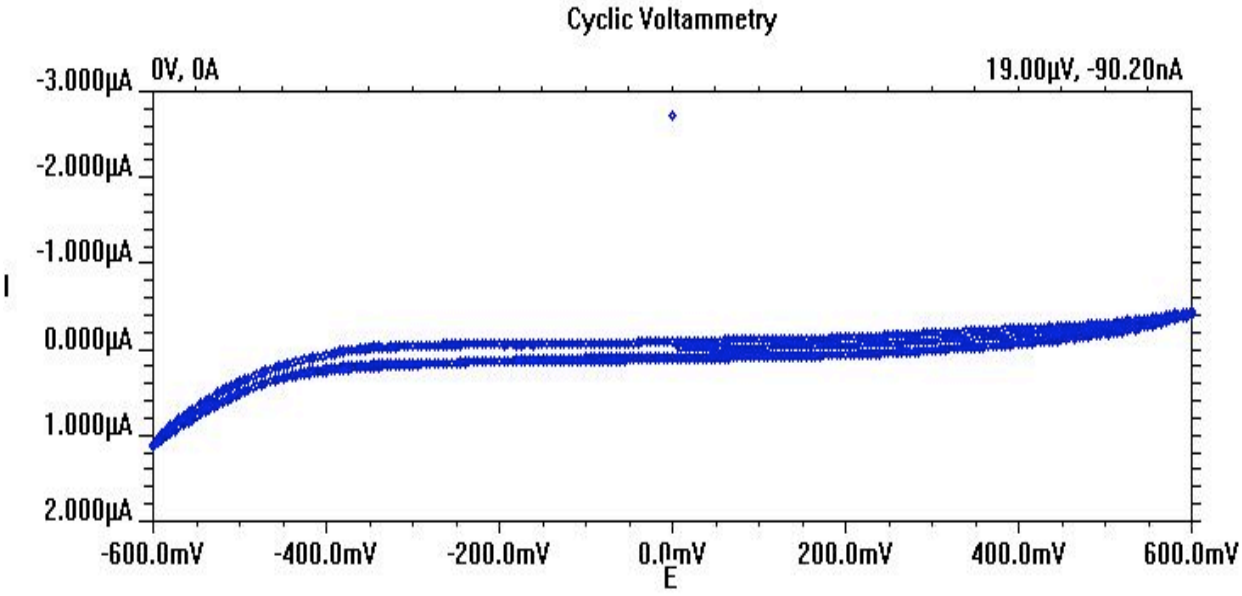

Figure 5. The low current and lack of peaks indicates that the carbon nanotubes are completely covered and insulated by polyphenol.

Figure 6. SEM Image of Carbon Nanotubes Coated with Polyphenol

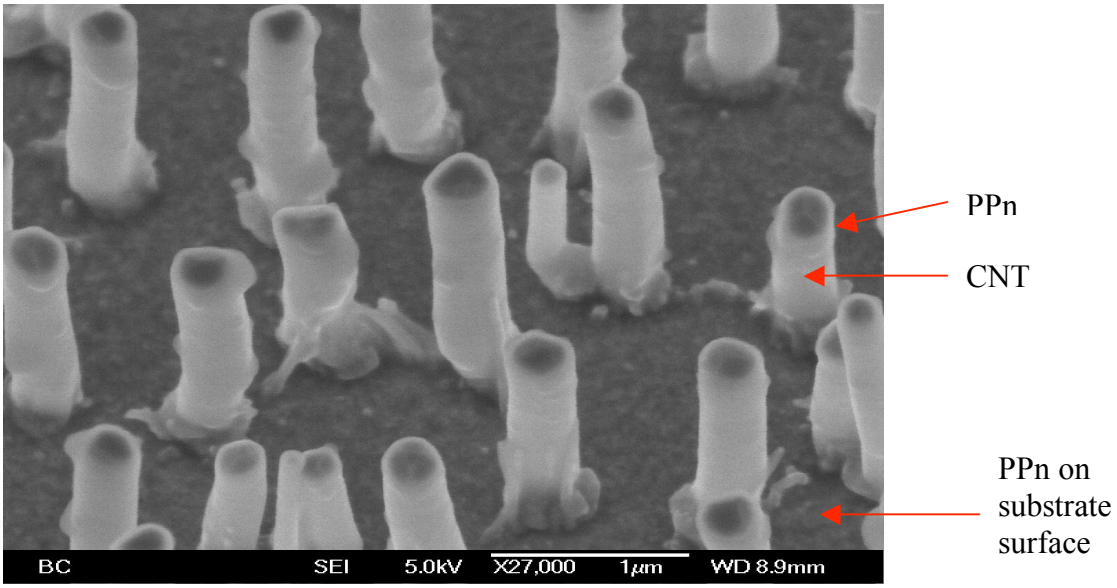

Figure 6. Vertically grown carbon nanotubes were coated electrochemically with PPn (white coating).

Figure 7. TEM Image of Carbon Nanotubes Coated with Ferritin Doped Polyphenol

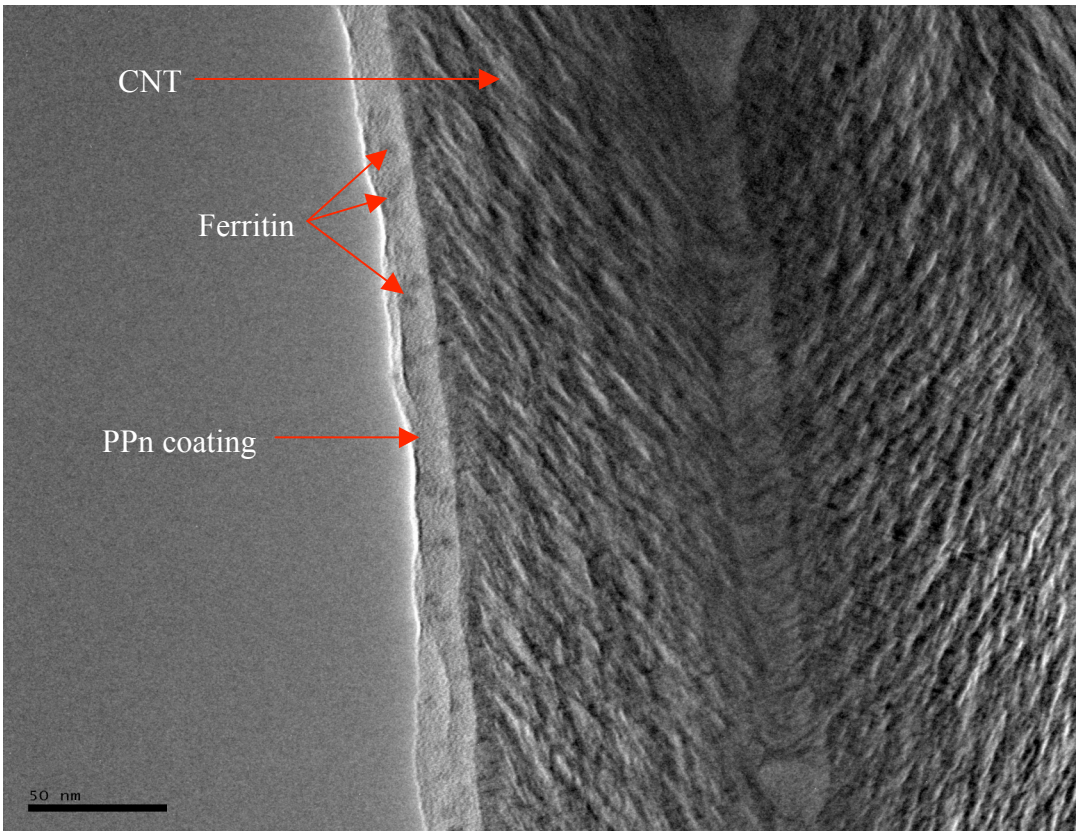

Figure 7. The textured portion on the right is the carbon nanotube. The light layer on the left on the left of the carbon nanotube is the polyphenol coating. The dark spots within the polyphenol are the ferritin molecules. (Scale bar = 50 nm)

Figure 8. PPn Stability Under Various Conditions

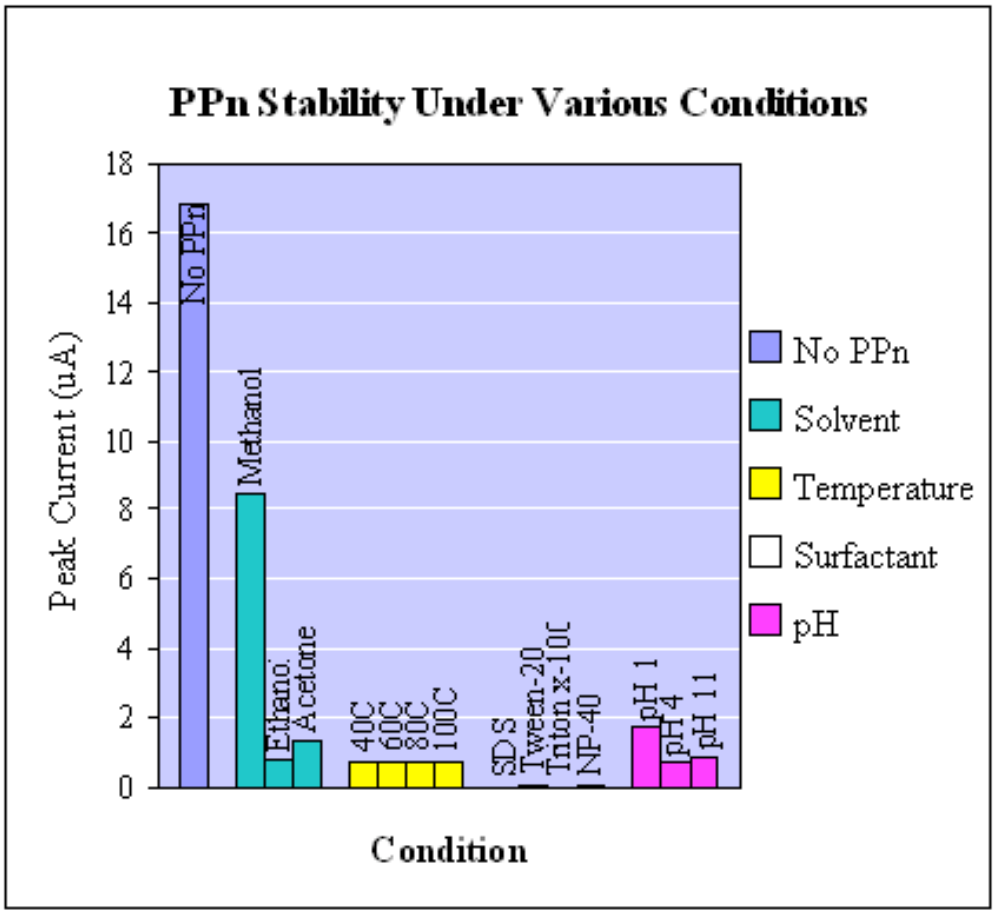

Figure 8. PPn without ferritin was deposited onto polished samples and developed in the solution indicated. After development cyclic voltammetry with FCA was conducted. The peak current value obtained was recorded and graphed. The bar labeled no PPn was a bare polished CNT array. The PPn coating was considered stable in any condition that yielded a value under 1µA. The PPn coating was considered unstable in any condition that yielded a value greater than 1 µA (methanol, acetone, and pH 1).

Figure 9. Hypothetical Results of Successful Ferritin Removal from Polyphenol

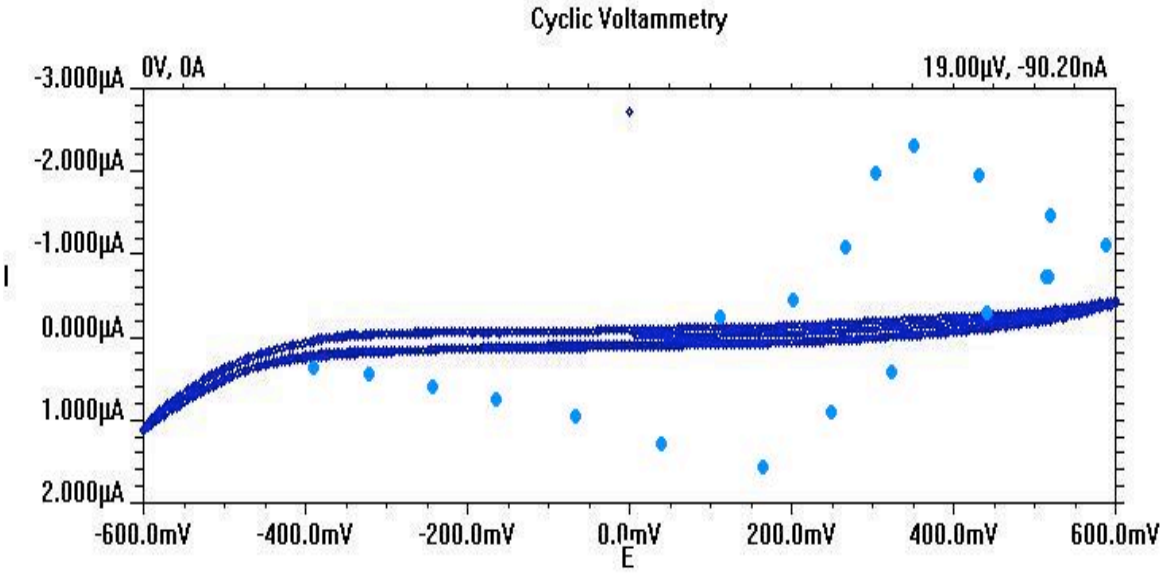

Figure 9. The light blue dots superimposed on the cyclic voltammetry plot after the polyphenol deposition are the expected results if the ferritin is successfully removed. Note scale as compared to Figure 4.

Figure 10. EIS Measurements of Molecularly Imprinted Sample During Fabrication

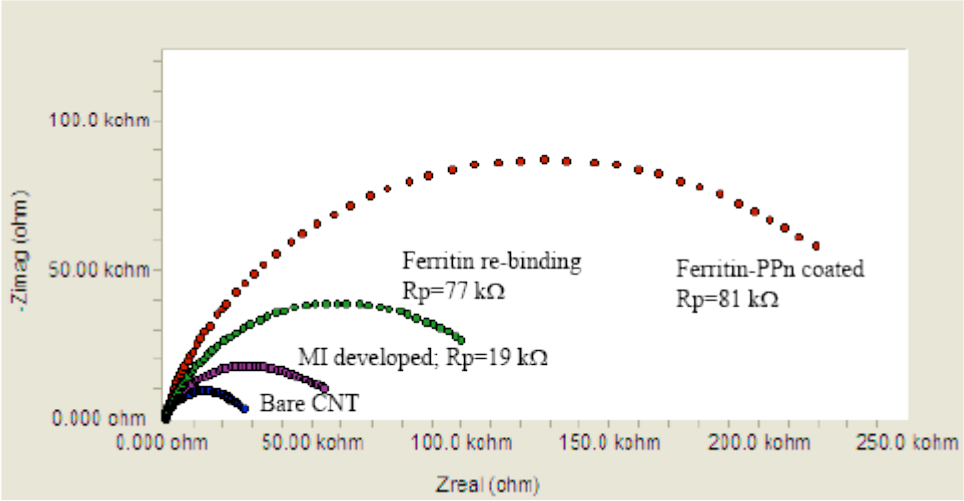

Figure 10. Blue – Impedance of carbon nanotube array before deposition.
Red – Impedance of carbon nanotube array after polyphenol/ferritin deposition.
Purple – Impedance of carbon nanotube array after development in 10% SDS / 10% acetic solution.
Green – Impedance of carbon nanotube array after reintroduction of ferritin.

Figure 11. EIS Measurements After Different Developing Solutions

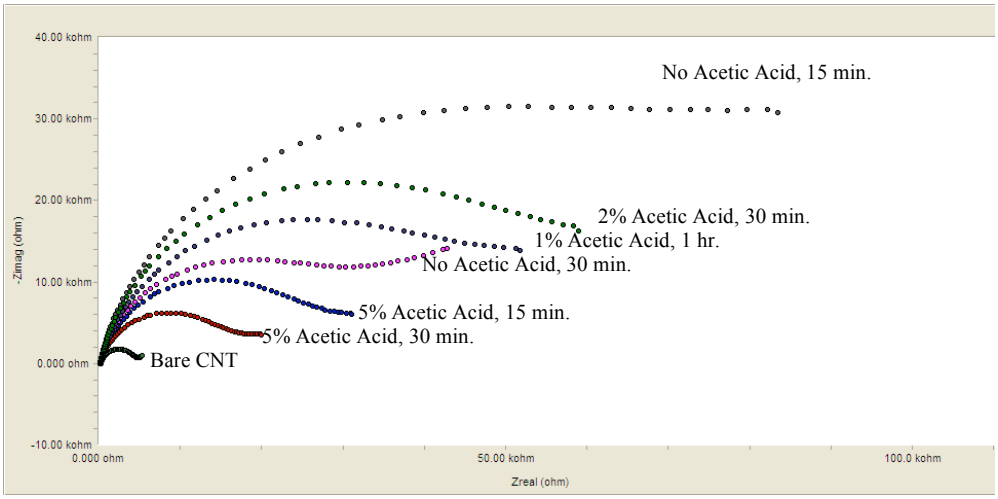

Figure 11. The above overlaid plots are the results of the different development conditions performed on multiple samples. All of the samples were developed with a combination of 10% SDS and the indicated acetic acid concentration for the indicated amount of time. While there is no visible trend relating acetic acid concentration and impedance it can be seen that the impedance decreases when the length of developing time is increased while keeping the acetic acid concentration fixed.

Figure 12. EIS Measurements Comparing Development with Deionized Water on Ferritin Doped and Ferritin Undoped PPn Samples.

a)

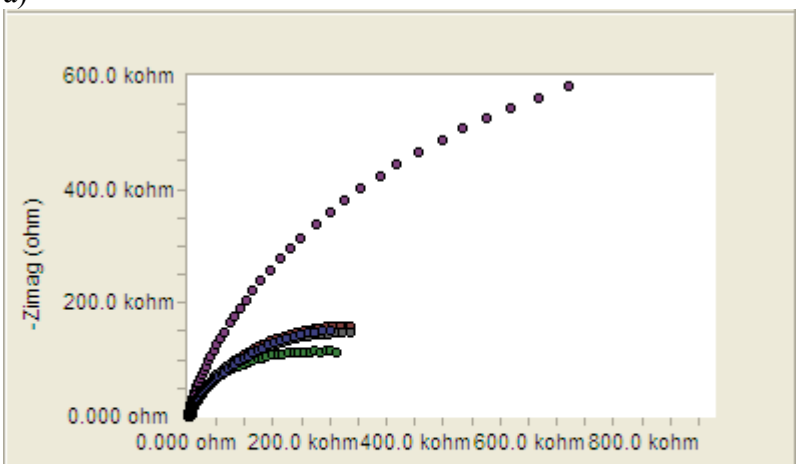

b)

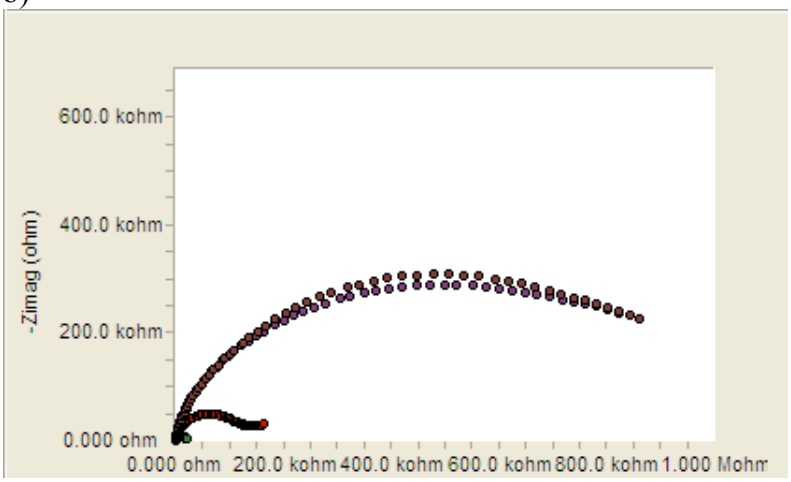

Figure 12. a) Purple – Impedance of ferritin doped PPn coating before development.
Green – Impedance after development with deionized water for 30 min.
Gray – Impedance after reintroduction of Ferritin at a concentration of 1 x 10^{-9} g/L.
Blue - Impedance after reintroduction of Ferritin at a concentration of 1 x 10^{-8} g/L.
Red - Impedance after reintroduction of Ferritin at a concentration of 1 x 10^{-7} g/L.
b) Green – Impedance of CNT array before deposition.
Orange – Impedance of PPn coating (no ferritin) before development.
Red – Impedance after development with 0.5% SDS for 15 min.
Purple – Impedance after development with deionized water for 15 min.

References

1. Haupt, K.; Mosbach K. Molecularly Imprinted Polymers and Their Use in Biomimetic Sensors. *Chem. Rev.* **2000**, *100,* 2495̃2504.

2. Hayden O.; Lieberzeit, P.; Blaas, D.; Dickert, F. Artificial Antibodies for Bioanalyte Detection—Sensing Viruses and Proteins. *Adv. Funct. Mater.* **2006**, *16*, 1269–1278.

3. Jakoby, B.; Ismail, G. M.; Byfield, M. P.; Vellekoop, M. J. A Novel Molecularly Imprinted Thin Film Applied to a Love Gas Sensor. *Sens. Actuators A.* **1999**, *76*, 93.

4. Chailapakul, O.; Crooks, R. Synthesis and Characterization of Simple Self -Assembling, Nanoporous Monolayer Assemblies: A New Strategy for Molecular Recognition. *Langmuir.* **1993***, 9,* 884-888.

5. Mirsky, V.; Hirsch, T.; Piletsky, S.; Wolfbeis, O. A Spreader-Bar Approach to Molecular Architecture: Formation of Stable Artificial Chemoreceptors. *Angew. Chem. Int. Ed*. **1999**, *38*, No. 8.

6. Piletsky, S.A.; Piletskaya, E.V.; Sergeyeva, T.A.; Panasyuk, T.L.; El'skaya, A.V. Molecularly Imprinted Self-Assembled Films with Specificity to Cholesterol. *Sensors and Actuators.* **1999**, *60*, 216–220.

7. Panasyuk, T. L.; Mirsky, V. M.; Piletsky, S. A.; Wolfbeis, O. S.. Electropolymerized Molecularly Imprinted Polymers as Receptor Layers in Capacitive Chemical Sensors. *Anal. Chem*. **1999**, *71*, 4609-4613.

8. Riskin, M.; Tel-Vered, R.; Willner, I. The Imprint of Electropolymerized Polyphenol Films on Electrodes by Donor-Acceptor Interactions: Selective Electrochemical Sensing of *N*,*N*′-dimethyl-4,4′-bipyridinium (Methyl Viologen). *Adv. Funct. Mater.* **2007**, *17*, 3858–3863.

9. Shi, H.; Ratner, B. D. Template Recognition of Protein-Imprinted Polymer Surfaces. *John Wiley & Sons, Inc*. CCC 0021-9304/00/010001-11.

10. Spinke, J.; Liley, M.; Schmitt, F.-J.; Guder, H.-J.; Angermaier, L.; Knoll, W. Molecular Recognition at Self-Assembled Monolayers: Optimization of Surface Functionalization. *J. Chem. Phys.* **1993**, *99*, 9.

11. Wang, Y.; Zhou, Y.; Sokolov, J.; Rigas, B.; Levonb, K.; Rafailovich, M. A Potentiometric Protein Sensor Built with Surface Molecular Imprinting Method. *Biosensors and Bioelectronics.* **2008** *24*, 162–166.

12. Gau, J.-J.; Lan, E. H.; Dunn, B.; Ho, C.-H.; Woo, J. C. S. A MEMS Based Amperometric Detector for E. Coli Bacteria Using Self-Assembled Monolayers. *Biosensors & Bioelectronics.* **2001**, *16*, 745–755.

13. Mengoli, G.; Musiani, M. M. An Overview of Phenol Electropolymerization for Metal Protection. *J. Electrochem. Soc*. **1987**, *134*, 12.

14. Gong, J.-L.; Gong, F.-C.; Zeng, G.-M.; Shen, G.-L.; Yu, R.-Q. A Novel Electrosynthesized Polymer Applied to Molecular Imprinting Technology. *Talanta*. **2003**, *61*, 447-453.

15. Feng, L.; Liu, Y.; Tan, Y.; Hu, J. Biosensor for the Determination of Sorbitol Based on Molecularly Imprinted Electrosynthesized Polymers. *Biosensors and Bioelectronics*. **2004**, *19*, 1513–1519.

16. Guerrieri, A.; Ciriello, R.; Centonze, D. Permselective and Enzyme-Entrapping Behaviours of an Electropolymerized, Non-Conducting, Poly(*o*-aminophenol) Thin Film-Modified Electrode: A Critical Study. *Biosensors and Bioelectronics*. **2008**, In Press.

17. Mahmoud, K. A.; Hrapovic, S.; Luong, J. H. T. Picomolar Detection of Protease Using Peptide/Single Walled Carbon Nanotube/Gold Nanoparticle-Modified Electrode. *ACS Nano*. **2008**, *2 (5*), 1051-1057.

18. Whitcombe, M. J.; Rodriguez, M. E.; Villar, P.; Vulfson, E. N. A New Method for the Introduction of Recognition Site Functionality into Polymers Prepared by Molecular Imprinting: Synthesis and Characterization of Polymeric Receptors for Cholesterol. *J. Am. Chem. Soc.* **1995**, *117*, 7105.

19. Wulff, G. Molecular Imprinting in Cross-Linked Materials with the Aid of Molecular Templates-A Way towards Artificial Antibodies. *Angew. Chem. Int. Ed. Engl.* **1995**, *34*, 1812-1832.

20. Vlatakis, G.; Andersson, L. I.; Müller, R.; Mosbach, K. Drug Assay Using Antibody Mimics Made by Molecular Imprinting. *Nature*. **1993**, *361*, 645-647.

21. Mosbach, K.; Ramström, O. The Emerging Technique of Molecular Imprinting and Its Future Impact on Biotechnology. *Bio/Technology*. **1996**, *14*, 163 -170.

22. Schweitz, L.; Andersson, L. I.; Nilsson, S. Capillary Electrochromatography with Predetermined Selectivity Obtained Through Molecular Imprinting. *Anal. Chem.* **1997**,*69*, 1179.

23. Sellergren, B. Direct Drug Determination by Selective Sample Enrichment on an Imprinted Polymer. *Anal. Chem.* **1994**, *66*, 1578.

24. Haupt, K.; Noworyta, K.; Kutner, W. Imprinted Polymer-Based Enantioselective Acoustic Sensor Using a Quartz Crystal Microbalance. *Anal. Commun.* **1999**, *36*, 391.

25. Chen, J.H.; Huang, Z.P.; Wang, D.Z.; Yang, S.X.; Li, W.Z.; Wen, J. G.; Ren, Z. F. Electrochemical Synthesis of Polypyrrole Films Over Each of Well-Aligned Carbon Nanotubes. *Synthetic Metals*. **2002**, *125*, 289-294.

26. Wang, S.G.; Zhang, O.; Wang, R.; Yoon, S. F. A Novel Multi-Walled Carbon Nanotube-Based Biosensor for Glucose Detection. *Biochemical and Biophysical Research Communications*. **2003**, *311*, 572–576.

27. Gao, M,; Dai, L.; Wallace, G. G. Biosensors Based on Aligned Carbon Nanotubes Coated with Inherently Conducting Polymers. *Electroanalysis*. **2003**, *15*, 13.

28. Malitesta, C.; Losito, I.; Zambonin, P. G. Molecularly Imprinted Electrosynthesized Polymers: New Materials for Biomimetic Sensors. *Anal. Chem.* **1999**, *71 (7)*, 1366-1370.

29. Turkewitsch, P.; Wandelt, B.; Darling, G. D.; Powell, W. S. Fluorescent Functional Recognition Sites Through Molecular Imprinting. A Polymer Based Fluorescent Chemosensor for Aqueous cAMP. *Anal. Chem.* **1998**, *70*, 2025.

30. Andersson, L.; Mandenius, C. F.; Mosbach., K. Studies on Guest Selective Recognition on an Octadecyl Silylated Silicon Surface Using Ellipsometry. *Tetrahedron Lett.* **1988**, *29*, 5437.

31. Kro¨ger, S.; Turner, A. P. F.; Mosbach, K.; Haupt, K. Imprinted Polymer-Based Sensor System for Herbicides Using Differential-Pulse Voltammetry on Screen-Printed Electrodes. *Anal. Chem.* **1999**, *71*, 3698.

32. Mosbach, K.; Andersson, L. I. Swedish Patent SE 9102843, **1991**.

33. Dickinson, T. A.; White, J.; Kauer, J. S.; Walt, D. R. A Chemical –Detecting System Based on a Cross-Reactive Optical Sensor Array. *Nature*. **1996**, *382*, 697.

34. Davis, J. J.; Coleman, K.; Azamian, B.; Bagshaw, C.; Green, M. L. Chemical and Biological Sensing with Modified Single Walled Carbon Nanotubes. *Chem. Eur. J.* **2003**, *9*, 3732.

35. Wang, J. Carbon-Nanotube Based Electrochemical Biosensors: A Review. *Electroanalysis*. **2005**, *17*, 1.

36. Baughman, R. H.; Zakhidov, A.; de Heer, W. A. Carbon Nanotubes – The Route Toward Applications. *Science*. **2002**, *297*, 787.

37. Ren, Z. F.; Huang, Z. P.; Xu, J. W.; Wang, D. Z.; Wen, J. G.; Wang, J. H.; Calvet, L.; Chen, J.; Klemic, J. F.; Reed, M. A. Growth of a Single Freestanding Multiwall Carbon Nanotube on Each Nanonickel dot. *Appl. Phys. Lett*. **1999**, *75*, 1086 -1088.

38. Sotiropoulou, S.; Chaniotakis, N. A. Carbon Nanotube Array-Based /biosensor. *Anal Bioanal Chem*. **2003**, *375*, 103–105.

39. Koehne, J.; Li, J.; Cassell, A. M.; Chen, H.; Ye, Q.; Ng, H. T.; Han, J.; Meyyappan, M. The fabrication and Electrochemical Characterization of Carbon Nanotube Nanoelectrode Arrays. *J. Mater. Chem*. **2004**, *14*, 676–684.

40. Li, J.; Stevens, R.; Delzeit, L.; Ng, H. T.; Cassell, A.; Han, J.; Meyyappan, M. Electronic Properties of Multiwalled Carbon Nanotubes in an Embedded Vertical Array. *Applied Physics Letters*. **2002**, ***81***, 5.

41. Lin, Y.; Lu, F.; Tu, Y.; Ren, Z. Glucose Biosensors Based on Carbon Nanotube Nanoelectrode Ensembles. *Nano Letters*. **2004**, *2*, 191.

42. Hawkins, D. M.; Stevenson, D.; Reddy, S. M. Investigation of Protein Imprinting in Hydrogel-Based Molecularly Imprinted Polymers (HydroMIPs). *Analytica Chimica Acta*. **2005**, *542*, 61–65.

43. Yu, Y.; Cimeno, A.; Lan, Y. C.; Rybczynski, J.; Wang, D. Z.; Paudel, T.; Ren, Z. F.; Wagner, D. J.; Qiu, M. Q.; Chiles, T. C.; Cai, D. Assembly of Multi-Functional Nanocomponents on Periodic Nanotube Array for Biosensors. **2009**, *4*, 27-33.